# Influence of Nonflat Plate Trailing Edge Serration on Airfoil Noise Reduction

C. K. Sumesh[1] and T. J. Sarvoththama Jothi[2]

**Abstract:** The current study experimentally investigates the influence of nonflat plate trailing edge serrations on airfoil noise characteristics. Experiments are carried out at different flow velocities in the range of 25–40 m/s, corresponding to the Reynolds number range of $2.4 \times 10^5$ to $3.9 \times 10^5$. The wavelength ($\lambda$) of the serrations considered is in the range of 5–30 mm, and the serration height ($2h$) is in the range of 10–30 mm. The acoustic spectra show that the conventional nonflat plate trailing edge serrations generate a narrowband vortex shedding noise. The narrowband noise is observed to decrease with an increase in the wavelength; however, it is observed to increase with an increase in the serration height or root thickness by around 16 dB. Inclinations ($\theta$) provided at the root of the serrations reduce the narrowband noise up to 20 dB and the broadband noise up to 5 dB. When a perforated plate inserts the sawtooth gap of the serration, the hybrid configuration effectively eliminates the vortex shedding phenomenon at the roots with a significant reduction in the low frequency range as well as the high frequency broadband noise. **DOI: 10.1061/JAEEEZ.ASENG-4995.** 

**Practical Applications:** Airfoil noise poses a significant challenge in aviation, wind energy, and other sectors where aerodynamic noise reduction are crucial. When an airfoil is subjected to turbulent flow, the primary source of noise arises from the interaction of the flow with its trailing edge. The geometrical modifications made at the trailing edge helps to minimize the intensity of the noise generation. This paper presents the results of an experimental investigation on the impact of nonflat plate trailing edge serrations. The major findings of the study reveal that employing a nonflat plate trailing edge serrations can substantially mitigate airfoil trailing edge noise levels.

**Author keywords:** Airfoil; Trailing edge noise; Serrations; Root thickness; Vortex shedding; Narrowband noise.



## Introduction

Noise generated from aircraft continues to exist as a major concern in the air transport industry, particularly in the development of airports in urban areas. One of the significant noises from an aircraft is the self-noise generated due to the interaction of flows with an airframe, particularly during landing and take-off. The noise generated from lifting devices and their mitigation have been a prominent field of research for several decades due to the complex nature of flow interaction. It is understood that a boundary layer over the trailing edge plays a vital role in noise generation (Brooks et al. 1989). The flow turbulence within the boundary layer generates pressure fluctuations on the airfoil surface, and when this pressure fluctuation passes over the sharp trailing edge, energy scattering occurs and generates noise. At lower Mach numbers, the trailing edge noise is significant due to the efficient scattering of the turbulent structures in the boundary layer (Williams and Hall 1970). The trailing edge noise can be reduced by altering the trailing edge geometry, thus the scattering efficiency. Various passive and active methods are used to minimize the trailing edge noise. The active methods include flow injection (Szoke et al. 2020b), suction (Szoke et al. 2020a), and plasma actuators (Inasawa et al. 2013), which require additional energy supply to the noise reduction system. However, due to the easiness of implementation, passive methods attract more importance. The most commonly employed passive noise reduction techniques include serrated trailing edge, porous treatments, trailing edge brushes, perforated extensions, and morphing surfaces. Albeit numerous noise mitigation methods exist, a serrated trailing edge ranks better in practicality and aerodynamic performance, as noted in the previous literature.

### *Flat Plate Serrations*

Howe (1991) analytically studied and identified that the serrations type of trailing edge geometry modification is one of the most efficient ways of reducing trailing edge noise. Howe's (1991) theory predicts that the serrations do not affect the low frequency noise generated by large eddies, while it predicts a substantial reduction in the high frequency noise. Moreover, to achieve noise reduction, the root-to-tip length of the serrations must be higher than the trailing edge boundary layer thickness. The experimental studies by Dassen et al. (1996), Parchen et al. (1999), Oerlemans et al. (2009), Gruber et al. (2010, 2011), and Chen et al. (2021) reported that an appreciable noise reduction of up to 7dB using trailing edge serrations at lower frequencies, however, noted higher noise levels at higher frequencies. Gruber et al. (2011) studied the effect of serration geometries on noise reduction using different serrations of various wavelength ($\lambda$) and serration height ($2h$). They obtained the noise reduction by 7 dB in a low frequency range of Strouhal number ($St_\delta < 1$) based on boundary layer thickness, while the noise increased up to 3 dB at higher frequencies due to the cross flow through the roots in the serration gap. Further, the hydrodynamic field near the serrated trailing edge largely influences noise

[1]Ph.D. Student, Dept. of Mechanical Engineering, National Institute of Technology Calicut, Kozhikode, Kerala 673601, India. Email: sumeshck@sctce.ac.in

[2]Associate Professor, Dept. of Mechanical Engineering, National Institute of Technology Calicut, Kozhikode, Kerala 673601, India (corresponding author). ORCID: https://orcid.org/0000-0002-9674-9045. Email: tjsjothi@nitc.ac.in

Note. This manuscript was submitted on December 1, 2022; approved on September 18, 2023; published online on December 26, 2023. Discussion period open until May 26, 2024; separate discussions must be submitted for individual papers. This paper is part of the ***Journal of Aerospace Engineering***, © ASCE, ISSN 0893-1321.

reduction. The maximum noise reduction is attained if the serration height is in the order of boundary layer thickness and the serration angle is small.

The experimental investigations carried out by Moreau and Doolan (2013) with trailing-edge serrations on a flat plate at low-to-moderate Reynolds numbers showed that the wake characteristics and the flow field at the trailing edge get modified by the sawtooth trailing edge. Therefore, they concluded that the noise reduction by the serrations is primarily due to the changes in the hydrodynamic field at the trailing edge rather than the change in the scattering efficiency of the trailing edge. Thus, they established that the frozen turbulence assumption is not effective in the case of a serrated trailing edge. Chong and Vathylakis (2015) experimentally examined the flow over trailing-edge serrations fitted to a flat plate. They found that the turbulence at the oblique edges, wall-pressure spectral density, and spanwise coherence do not vary significantly by the serration. However, substantial noise reduction is obtained at midfrequencies by sweeping the vortical structures concentrated near the serration tip to the serration side edges due to the interaction of the pressure-driven vortices. Therefore, the noise decrease is attributed to the reduction in the scattering efficiency related to the oblique edges and not due to the decrease in source strength. Later, the experimental investigations by Arce León et al. (2016) and Avallone et al. (2016) further substantiated the conclusions of Chong and Vathylakis (2015). They showed that the intensity of the pressure fluctuations decreases from root to tip. By analyzing the time-resolved particle image velocimetry (PIV) data, Avallone et al. (2016) proved that the low frequency noise is produced at the roots of the serration, whereas the higher frequency noise is generated at the tips. A serrated flat plate extension with flap angle should affect the cross-jet at the serration root and the resulting trailing edge noise reduction. Vathylakis et al. (2016) observed that the flap-up position of the serration could produce a better noise reduction of around 2dB at high frequencies than the flap-down position.

The semi-analytical model developed by Lyu et al. (2016) more accurately predicts noise reduction by trailing edge serration than Howe's model. They suggested another possible mechanism for noise reduction in which the destructive interference of the pressure waves scattered along the serration edge. However, some discrepancies regarding the noise measurements still prevail due to the frozen turbulence assumption. The theory of destructive interference has been further established by Van der Velden et al. (2017). This noise reduction model suggests that the important parameter to ensure sufficient noise reduction is that the serration must have enough height to produce an effective phase difference among the scattered pressure waves. Singh et al. (2022) experimentally investigated the efficiency of sinusoidal trailing edge serrations as a method to reduce the broadband noise. They observed that longer sinusoidal serrations provide higher noise reductions as compared to the shorter serrations irrespective of its wavelengths. They also reported that the trailing edge sinusoidal serrations reduce the leading-edge turbulence interaction noise along with the airfoil self-noise, thus obtaining an overall noise reduction. In all the mentioned cases, the serrations were made in a flat plate and retrofitted to the airfoil's trailing edge. Hu et al. (2022) carried out a numerical study to investigate the flow past NACA-0012 airfoil with different flat plate trailing edge serrations and serration edge profiles at zero incidence. Results demonstrate that the destructive interference is the primary mechanism for noise reduction, and the serration's shape play a significant role in the destructive interference. The noise reduction mainly occurred in the low- and midfrequency ranges, and the feather-like serrations resulted in better noise reduction compared to other models.

### *Nonflat Plate Serrations*

Chong et al. (2013a) conducted an experimental study on the acoustic characteristics of a nonflat plate–type serrated trailing edge with different serration parameters. The measured noise spectra showed a reduction of 2–8 dB compared to the baseline airfoil. However, a tonal peak in a narrow frequency band is observed due to the bluntness at the sawtooth root. They attempted to reduce the bluntness-induced vortex shedding by covering the nonflat plate serrated trailing edge portion using a woven-wire mesh screen; however, it was only partly successful. The effect of different nonflat plate serration geometries on instability noise and broadband noise reduction is reported by Chong et al. (2013b). A serration with a larger serration angle and smaller height is recommended to obtain a moderate self-noise reduction. They also concluded that weakening the strength of vortex shedding provides additional noise benefits.

It is important to understand the effect of nonflat plate trailing edges in the hydrodynamic flow developed over an airfoil and the near wake structures for understanding the noise reduction effects. The studies by Hasheminasab et al. (2021) and Thomareis and Papadakis (2017) explain the flow behavior of narrow and wide serrations, respectively. The PIV results of Hasheminasab et al. (2021) showed that no substantial difference in the wake momentum deficit at the root and tip of the narrow serrations. The von Karman like vortex shedding occurring at the roots with a convection velocity of 90% of the free stream velocity ($U_\infty$). They also showed that the periodic vortex shedding at the root plane has no interaction with flow structures in a spanwise direction. In contrast, for the wide-angle serrations, Thomareis and Papadakis (2017) showed that the wake deficit is higher at the tip of the serration than that at the root because of the secondary flow developed in the space between the teeth of the serration. The three-dimensional (3D) flow causes a spanwise inhomogeneity, which decreases the spanwise coherence during the vortex shedding. The vortex shedding tones of the blunt trailing edge and bluff bodies observed to increase the frequency and broaden the bump with an increase in speed and decrease in characteristic length (Schlinker et al. 1976). Howe (1976) analyzed the influence of vortex shedding on sound generation in a two-dimensional field by the convecting turbulent eddies in mean flow past a trailing edge of a compact airfoil/semi-infinite plate. It is shown that the far-field mean square sound pressure varies with fifth power of the flow velocity.

Vathylakis et al. (2015) conducted experiments using airfoil with nonflat plate type trailing edge serrations with different types of porous materials filled in the gap between adjacent sawtooth to suppress the bluntness vortex shedding noise. Different types of porous metal, synthetic foams, or thin brush bundles were used to fill the serration gaps. They reported that a solid serration with a permeable material to fill the serration gap significantly reduces the broadband and vortex shedding tonal noise levels. Later, Chong and Dubois (2016) investigated the different poro-serrated trailing edge configurations with the same serration geometry and various porous materials with different flow resistivities to fill the sawtooth gap. They found that a porous material of low-flow resistivity did not completely suppress the vortex shedding noise, but it attains a reasonably good broadband noise reduction at high frequency. On the other hand, no vortex shedding tone exists when the sawtooth gaps are filled with very high-flow resistivity porous material. However, an optimal flow resistivity at the serration gap further enhances the broadband noise reduction. The experimental investigations by Nedić and Vassilicos (2015) and Prigent et al. (2017) in a nonflat plate sawtooth trailing edge and nonflat plate sinusoidal serrations, respectively, showed that employing a fractal/multiscale

pattern to the oblique edge of the nonflat plate serration reduces the turbulent energy and the spanwise coherence of the vortex shedding. Further, the acoustic study carried out by Hasheminejad et al. (2018) established that the multiscale/fractal pattern at the slant edge of the cut-in serrated trailing edge significantly reduces the tonal noise due to the bluntness-induced vortex shedding. The experimental results of Celik et al. (2021) showed that the destructive interference of the scattering noise sources along the serration edge helps to achieve broadband noise reduction. It is also revealed that the presence of oblique vortical structures along the sawtooth slant edges interact with the turbulent boundary layer and ultimately results in the reduction of broadband noise.

### *Objectives*

It is evident from the literature that flat plate serration provides a sufficient noise reduction. However, its lower strength and aerodynamic performance, vibration, and safety issues might be a concern for practical implementation (Chong et al. 2013a, b). In addition, the noise reduction efficiency of the flat plate serration depends on the flap angle (Arce León et al. 2016; Vathylakis et al. 2016) and increases the noise levels in higher frequencies (Oerlemans et al. 2009; Gruber et al. 2011). To overcome these drawbacks, nonflat plate trailing edge serrations are considered for the present study. A few theoretical and experimental works on nonflat plate serration airfoils concluded that the inclined serration edge is responsible for reducing the scattering noise (Howe 1991; Lyu et al. 2016; Chong et al. 2013b; Celik et al. 2021), thus making it beneficial for turbulent boundary layer noise reduction applications. Importantly, the usage of nonflat serrations will lead to the generation of narrowband noise due to vortex shedding from its blunt root, and thus requires a detailed parametric study. An immediate challenge of using such serrations is to mitigate the narrowband noise while retaining the serration's benefits at other frequencies, which is noted as a lacuna in the literature. Therefore, the usage of an appropriate passive methods to mitigate the narrowband noise in nonflat serrations airfoil is the novel aspect in this paper. The objectives of the work are described as follows. Initially, the noise characteristics of blunt root serrations with variations in the wavelength ($\lambda$) and serration height ($2h$) are discussed. Second, an attempt is made to reduce the narrowband tonal noise from the blunt root of nonflat serrations by varying the (1) root inclination, and (2) inserting a perforated plate between the serration gap.

## Experimental Methodology

The acoustic measurements were carried out in a semi-anechoic open jet test facility. The open jet wind tunnel test section was situated in the semi-anechoic chamber of $2.6 \times 2.6 \times 2.6$ m to facilitate the acoustic measurements. The cut-off frequency of the anechoic chamber was measured as 300 Hz, above which the chamber ensures a reverberation-free environment. The test facility contained a three-dimensional contraction nozzle outlet with a rectangular cross section with dimensions of 0.08 m in height and 0.20 m in width, as shown in Fig. 1(a). The airstream velocities considered for investigations were in the range of 25 to 40 m/s, and the corresponding Reynolds numbers ($Re_c$) based on the chord ($c$) were in the range of $2 \times 10^5$ and $4 \times 10^5$. The turbulent intensity of the flow measured at the center of the nozzle exit plane was around 0.2%, and the side plates were placed outside the air steam. Thus, the radiated noise from the airfoil was mainly generated from the trailing edge of the airfoil. The background noise of the facility as well below the self-noise of the airfoil at all velocities (Sumesh and Jothi 2021). The airfoil was mounted horizontally with the leading edge at a distance of 25 mm from the nozzle exit plane and was held by the side plates attached to the nozzle lips [Fig. 1(b)]. The geometric angle of attack of the airfoil was set to zero degrees with the jet flow direction. The midfield noise measurements were carried out by a quarter-inch condenser microphone (PCB 378C01) placed at a distance of 0.6 m vertically above the midspan of the trailing edge. The acoustic data was acquired at a sampling frequency of 150 kHz using a 16-bit Analog-Digital card (NI PCI-6143) using LabView software version 2015. Timeseries data was captured for six seconds and processed for power spectral density (PSD) using *Welch's* function in MATLAB version R2016a and a Hanning window of a sample size of 4,096 and 50% overlap, resulting in a bandwidth resolution of 36.6 Hz.

A NACA0012 airfoil with a chord length ($c$) of 0.15 m and span of 0.3 m was used for the present study. In order to attach the various

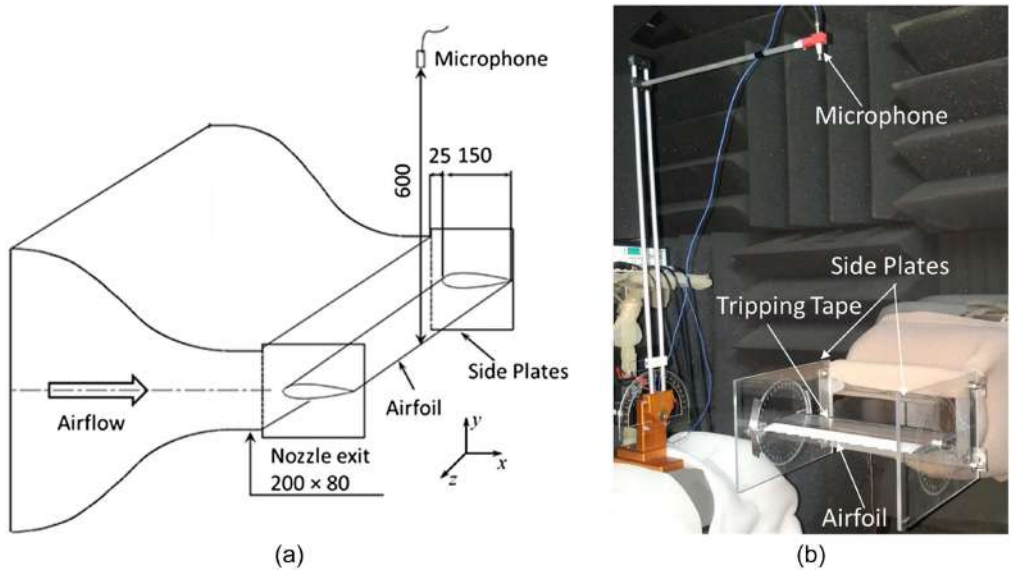


**Fig. 1.** (a) Schematic of the experimental setup (all dimensions in mm); and (b) photograph of experimental setup.

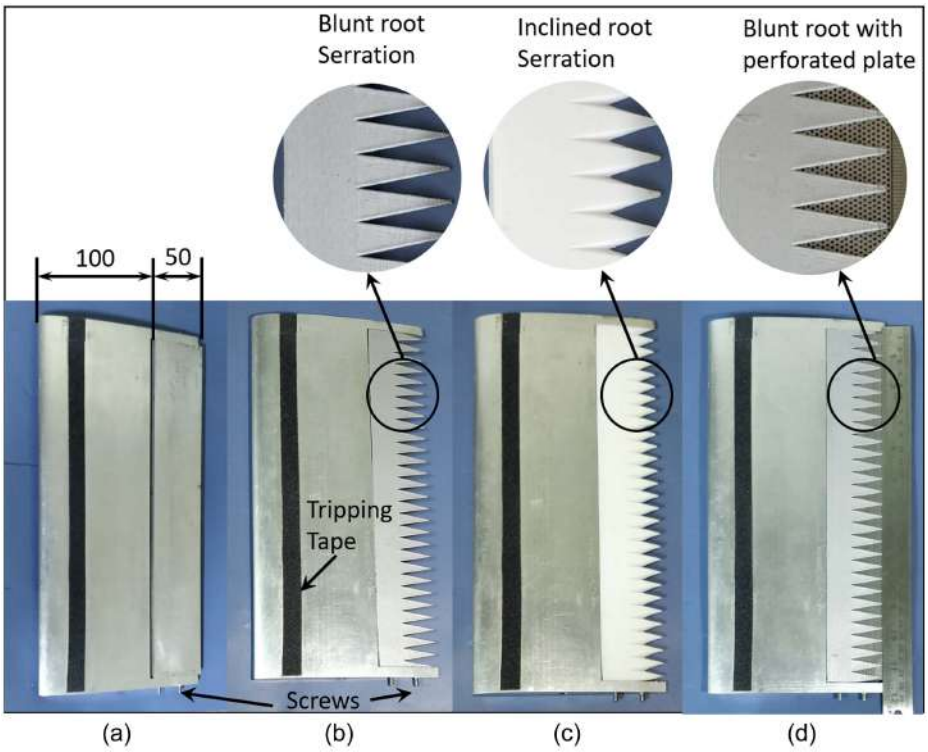


**Fig. 2.** NACA0012 airfoil test model with serrations: (a) base model; (b) blunt root serration; (c) inclined root serration; and (d) blunt root with perforated plate (all dimensions in mm).

trailing edge models, the airfoil was fabricated as two parts, namely the main body and trailing edge part, as shown in Fig. 2. The main body portion was from the leading edge ($x/c = 0$) to $x/c = 0.67$, and as made of aluminum material. The trailing edge portion was between $x/c = 0.67$ and $x/c = 1$, and was 3D printed in polylactic acid. The different trailing edges were attached to the main body using screws at the span edges, as shown in Fig. 2. The boundary layer over the airfoil was tripped by a rough tape (Fig. 2) of thickness 0.7 mm adhered along the span at $0.3c$ from the leading edge to ensure a turbulent boundary layer without losing the lift to drag ratio of airfoil (Giguere and Selig 1999). Three models were investigated and compared with the base model (without serrations). Fig. 2(b) shows the serrations with a blunt root thickness. Figs. 2(c and d) represent the serration with an inclined root and serration with a perforated plate, respectively. Fig. 3(a) shows the schematic of the trailing edge serration model with different geometric parameters such as serration wavelength ($\lambda$), serration height ($2h$), serration angle ($\varphi$), root thickness ($\varepsilon$), and root inclination ($\theta$). To investigate the first objective, the geometrical parameters of the blunt root serrations considered are summarized in Table 1. In the first case of the study (Case I in Table 1), serrations of different wavelengths of $5 \leq \lambda \leq 30$ and the same $2h$ and $\varepsilon$ were considered. In the second case (Case II), the wavelength was maintained constant and the serrations height varied. For investigating the second objective, two types of serrations were fabricated with modifications at the root, one with an inclined root [Fig. 2(c)] and the other with a perforated plate inserted in between the serration along the span [Fig. 2(d)]. The inclinations ($\theta$) were made at the root with respect to the mean flow direction so as to ensure a smooth flow over it and avoid vortex shedding [Fig. 3(b)]. Serrations with two different root inclinations, namely, 40° and 23° were considered. The serration height was $2h = 30$, and different wavelengths of $5 \leq \lambda \leq 30$. To investigate the effect of perforation along with the serrations, a perforated plate of an open area

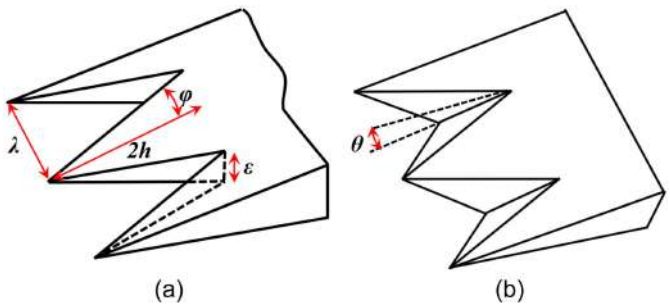


**Fig. 3.** Schematic of different solid serrations: (a) blunt root; and (b) inclined root.

**Table 1.** Geometric properties of the serrations of trailing edge

| Serration models | $\lambda$ (mm) | $2h$ (mm) | $\varepsilon$ (mm) | $n$ (power law index) |
|---|---|---|---|---|
| Baseline | 0 | 0 | 0 | — |
| Case I | 5 | 30 | 7.7 | 4.9 |
| | 10 | | | 5.5 |
| | 15 | | | 6.6 |
| | 20 | | | 6.5 |
| | 25 | | | 6.5 |
| | 30 | | | 5.9 |
| Case II | 10 | 30 | 7.7 | 5.5 |
| | | 20 | 5.7 | 4.6 |
| | | 10 | 2.8 | 4.3 |

ratio of 38.86%, 0.6 mm thickness, and $2h = 30$ was inserted along the span [Fig. 2(d)].

## Results and Discussions

This section describes the acoustic results of an airfoil attached to the different types of serrations and compares it with the base model airfoil at different flow velocities. Measurements were carried out at zero angles of attack for different freestream velocities in the range of 25 m/s to 30 m/s, corresponding to the Reynolds number range of $2 \times 10^5$ to $4 \times 10^5$. First, the spectral results are presented to demonstrate the effect of nonflat plate (blunt root) serrations on the radiated noise from the airfoil and discuss the characteristics of the noise components like the tonal noise in the spectra. This is followed by the comparison of noise spectra and noise reduction of blunt root serration and the modified serrations.

### *Noise Emissions from Blunt Root Serrations*

The acoustic spectra of the different blunt serration airfoils for wavelengths of $5 \leq \lambda \leq 30$ and $2h = 30$ (Case I) are shown in Fig. 4 for a free stream velocity of 40 m/s. It is understood from the figure that the serrations are effective in reducing the broadband noise in the lower frequency region of $300 \leq f \leq 600$ Hz and higher frequency region of $1{,}350 \leq f \leq 5{,}000$ Hz compared to that of the base model airfoil ($\lambda = 0$). The maximum noise reductions are observed to be around 2.6 dB and 5 dB. The noise in the frequency band of $300 \leq f \leq 600$ Hz could be due to the jet noise and its interaction with the leading edge (van der Velden et al. 2017). The higher frequency region ($1{,}350 \leq f \leq 5{,}000$ Hz) represents the turbulent boundary layer (TBL) scattering noise and is observed to not vary with the wavelength. However, comparing the base model airfoil, the serrations effectively alter the flow mechanism responsible for the TBL scattering noise generation. The secondary flow generated between the serration gap and its misalignment demonstrates the effect of serrations in reducing the TBL scattering noise (Avallone et al. 2016). Further, the reduced coherence of the spanwise velocity component at higher frequencies also attributes to the TBL scattering noise in this frequency range (Howe 1991). As expected, an intense tonal noise in the frequency band of $600 \leq f \leq 1{,}350$ Hz is observed due to the bluntness at the serration root leading to the vortex shedding (Chong et al. 2013b). It is noticed from Fig. 4 that the peak tonal frequency increases with an increase in the wavelength ($\lambda$), and their tonal noise levels are seen to decrease. However, for $\lambda \geq 25$, the tonal frequency and tonal amplitude are observed to be identical. The variation in the tonal frequency is noted, albeit the root thickness of the serrations is the same. Therefore, it is expected to depend on the serration wavelength. The higher tonal frequency at a larger $\lambda$ is due to the effect of three-dimensional flow at the root and a significant wake deficit at the tip of the serration than that at the root (Hasheminasab et al. 2021; Thomareis and Papadakis 2017). These three-dimensional flows cause spanwise inhomogeneity and decrease the vortices spanwise coherence. Thus, this secondary flow at the root reduces the tonal noise levels at a larger wavelength $\lambda$. The lower tonal frequency of the narrow serrations (smaller $\lambda$) is depicted to the fact that there is no substantial difference in the wake momentum deficit at the root and tip, and a Karman like vortex shedding exists at the root (Hasheminasab et al. 2021). Moreover, the bandwidth of the tonal noise is almost the same. It is also noted that the vortex shedding phenomenon at the root does not affect the TBL scattering noise in the frequency band of $1{,}350 \leq f \leq 5{,}000$ Hz. Similarly, the higher noise levels in the case of the smallest serration wavelength are due to the fact that the higher number of blunt roots along the span reduces the strength of the secondary flow. Hence the vortex shedding at the root is more coherent, which leads to a narrow peak with a higher sound pressure level (SPL).

Fig. 5 shows the spectra of airfoils with trailing edge serrations of different heights ($2h = 10$, 20, and 30) and $\lambda = 10$ mm (Case II in Table 1). The increase in the height of the serration causes an increase in the serration root bluntness $\varepsilon$. In this case, the tonal frequency peak decreases with an increase in $2h$, while the tonal amplitude increases. It is observed that the decrease in the serration height broadens the tonal frequency bandwidth. This may be due to the increase in the root thickness $\varepsilon$ with an increase in serration height. Therefore, with an increase in root thickness, the tonal peak noise levels increase and the tonal frequency decreases. This also corroborates with the findings of Tam and Ju (2012), where a thicker trailing edge would produce a lower tone frequency with higher noise levels than a thinner trailing edge. The serration with a thick blunt root tends to generate higher vortex shedding

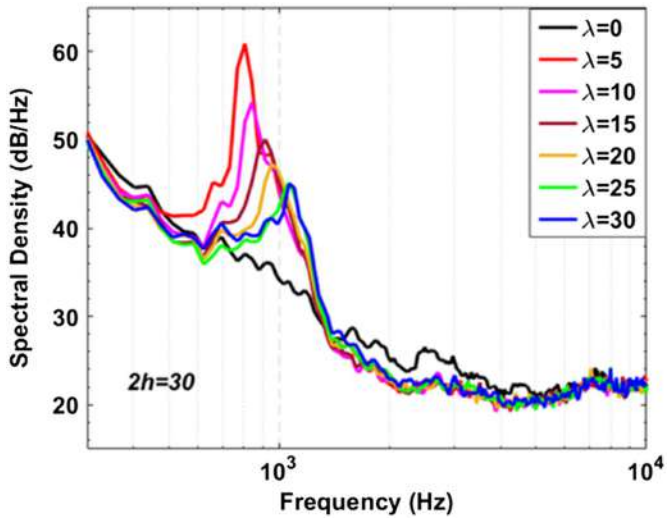


**Fig. 4.** Spectra of blunt root serration for various values of $\lambda$ and $2h = 30$ at $U_\infty = 40$ m/s.

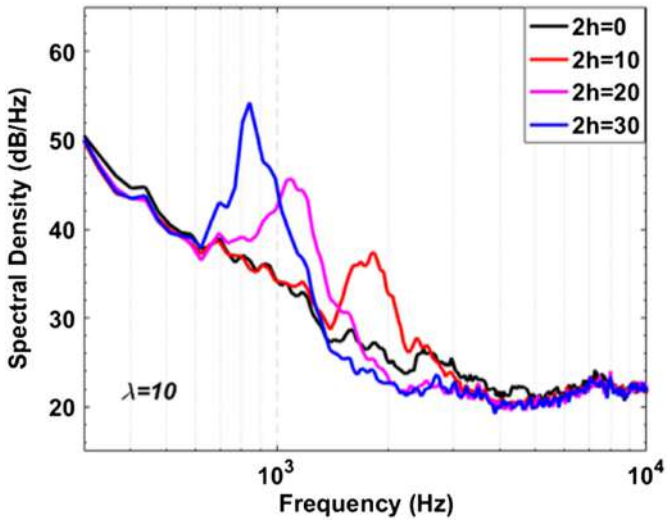


**Fig. 5.** Spectra of blunt root serration for various values of $2h$ and $\lambda = 10$ at $U_\infty = 40$ m/s.



J. Aerosp. Eng., 2024, 37(2): 04023122

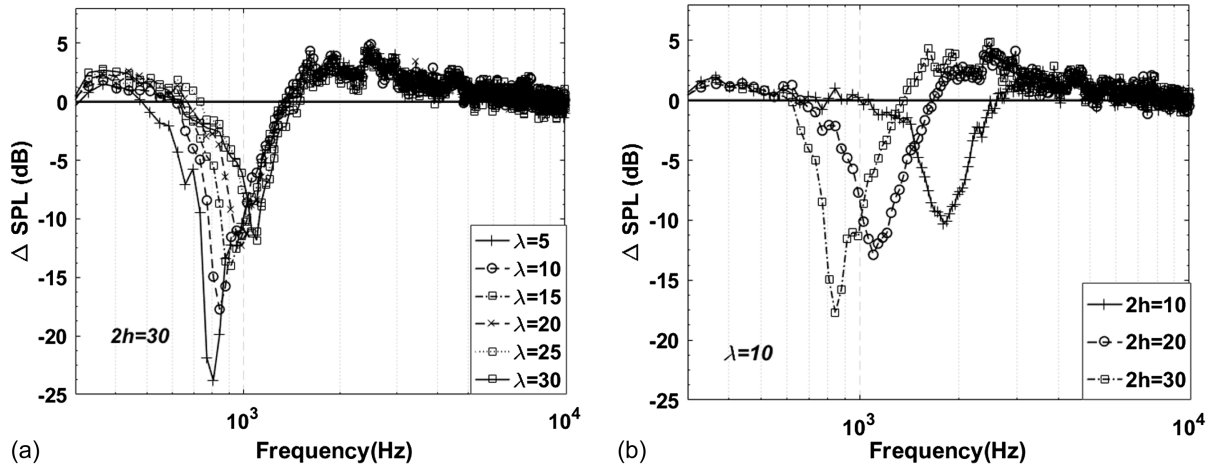


**Fig. 6.** ΔSPL spectra of different blunt root serrations at $U_\infty = 40$ m/s for (a) $2h = 30$ and different $\lambda$; and (b) $\lambda = 10$ and different $2h$.

noise in a lower frequency than a thinner root serration due to an increase in the magnitude of quadrupole sources near the serration root (Arias Ramírez and Wolf 2015).

Figs. 6(a and b) represents the ΔSPL spectra of different blunt root serration at $U_\infty = 40$ m/s corresponding to the configurations shown in Figs. 4 and 5, respectively. The ΔSPL is calculated by subtracting the SPL of the serrated airfoil from the base model airfoil, given by Eq. (1)

$$\Delta\text{SPL} = \text{SPL}_{\text{base model}} - \text{SPL}_{\text{serration model}} \tag{1}$$

The positive value of ΔSPL represents the noise reduction, and the negative value represents the noise increase compared to the base model airfoil. A maximum of 2.6 dB reduction in noise is obtained in the frequency range of $300 \le f \le 600$ Hz. An increase in the SPL reduction is observed with a gradual increase of serration wavelength ($\lambda$), and the widest serration ($\lambda = 30$) provides a maximum noise reduction in this frequency range, as shown in Fig. 6(a). The reduction in SPL is caused by the change in the flow field due to the vortex shedding occurs at the roots of the serration. At the roots of the serration, large-scale vortex shedding occurs, while at the tip, no vortex shedding is likely to occur due to the sharpness of the tip. Consequently, the presence of the strong vortex shedding develops a nonhomogeneous flow field at the trailing edge in the spanwise direction, results in the distortion of the upstream stagnation point along the span of the airfoil. Therefore, jet flow hitting the leading edge cannot remain two-dimensional and hence reduce the spanwise coherence at the leading edge, leading to the reduction of leading-edge interaction noise (Chong and Dubois 2016). The serrations in the frequency region of $600 \le f \le 1{,}350$ Hz increases the noise levels from 11 to 23 dB with a decrease in the serration wavelength, as shown in Fig. 6(a). In Fig. 6(a), the frequency range $1{,}350 < f < 5{,}000$ Hz represents the frequency range where a substantial reduction in broadband trailing edge noise is observed. A maximum of 5 dB reduction can be observed for all serrations considered. In the higher frequency band of $5{,}000 < f < 10{,}000$ Hz, the ΔSPL is zero signifying the neutral effect of the serrations in the airfoil [Figs. 6(a and b)].

Fig. 7 shows the variation of the Strouhal number based on the tonal frequency in the range of $600 \le f \le 1{,}350$ Hz (Fig. 4) and root thickness with serration angle ($\lambda/2h$). The Strouhal number is given by Eq. (2)

$$St_\varepsilon = \frac{f\varepsilon}{U_\infty} \tag{2}$$

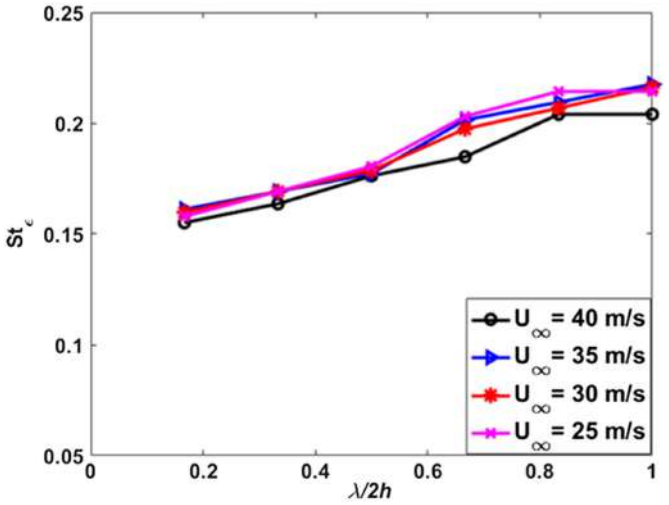


**Fig. 7.** Variation of Strouhal number with serration angle ($\lambda/2h$).

The Strouhal number is observed to collapse in the range of 0.15 to 0.2, depicting the range of vortex shedding Strouhal number, and is corroboration with the results of Nedić and Vassilicos (2015). Generally, a flat back airfoil with a constant root thickness along the span would show a constant Strouhal number with velocity (Brooks et al. 1989). However, in the present case, the Strouhal number increases with an increase in $\lambda/2h$ albeit the root thickness is constant. The wider serration has a larger Strouhal number, and the narrow serration has a lower Strouhal number and is in good agreement with the study of Chong et al. (2013b). The higher value of the Strouhal number for larger $\lambda$ is due to the effect of three-dimensional flow at the root, as explained in the previous section (Hasheminasab et al. 2021; Thomareis and Papadakis 2017).

Fig. 8(a) shows the variation of peak tonal SPL as a function of velocity and Mach number for serration models of different wavelengths. Generally, the vortex shedding noise levels can be represented as a function of velocity with a power law, whose indices denote a weak or strong dependency on the jet velocity. Theoretically, the sound pressure levels of a vortex shedding noise manifest a fifth power dependence on Mach number (Liu et al. 2017; Tam and Ju 2012), as shown in Eq. (3)

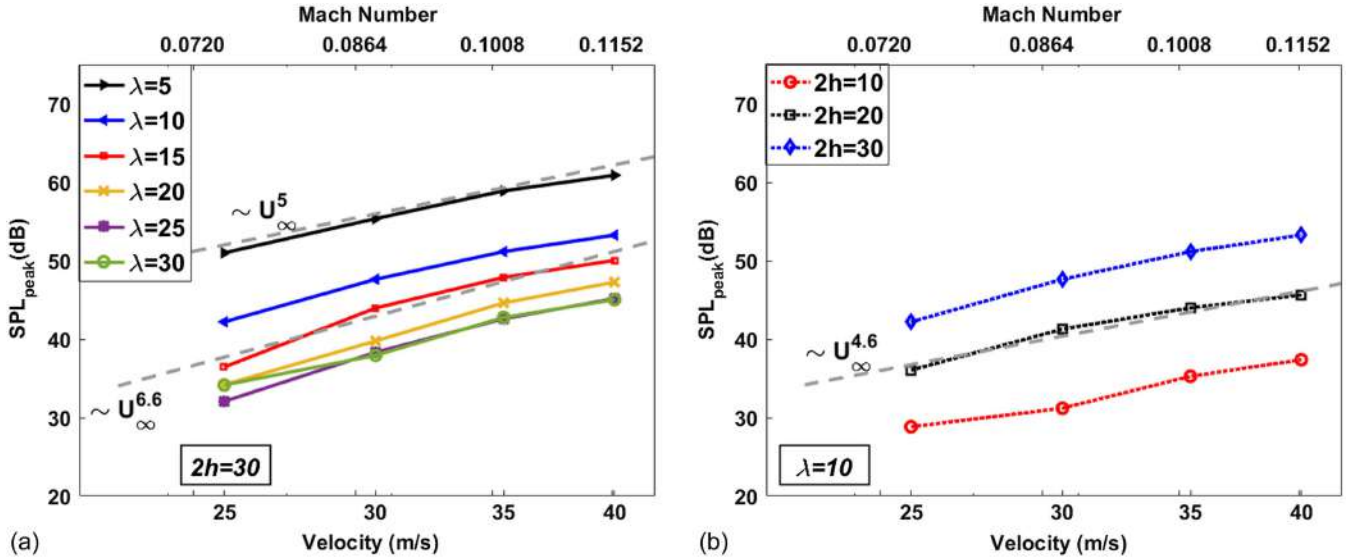


**Fig. 8.** Variation of narrow band peak SPL with velocity and Mach number for (a) $2h = 30$ and different $\lambda$; and (b) $\lambda = 10$ and different $2h$.

$$\overline{P^2} \sim M^5 (l/R) \sin^2 \phi \tag{3}$$

where $M$ = flow Mach number; $l$ = characteristic length of a sound source; $R$ = shortest distance of the microphone position from the sound source; and $\phi$ = polar position of the observer. The present results show a different scaling compared to that of the theoretical scaling by Howe (1976). The power law indices of the different serrations are presented in Table 1. The serration with the lowest wavelength ($\lambda = 5$) exhibits the strongest vortex shedding. Thus, the SPL scaling is very close to the fifth power $U_\infty^5$ (Fig. 8). This reveals that this tonal noise is similar to that of a blunt trailing edge, and the spanwise coherence of the vortex shedding is not affected by the presence of serrations. However, the peak tonal noise levels of the other serration airfoils scale with a higher power law index in the range of $U_\infty^5 - U_\infty^{6.6}$. This reveals a shift in the scaling factor with an increase in the serration wavelength. The increase in the power law index with the wavelength indicates a weaker dependence of the dipole source with the velocity, which could be due to the secondary flow in the serration gaps and weakening the longitudinal vortex shedding. Fig. 8(b) represents the variation of peak tonal SPL as a function of velocity and Mach number for serration models of different heights. As the serration height decreases, the noise dependence is proportional to $U_\infty^{4.6}$, where the power law index is lower than the theoretical value. The lower value of the index implies that the acoustic wavelength of the noise generated is lower than that of the former case with a longer serration height, and the airfoil is acoustically noncompact at this comparatively higher frequency (Powell 1959). At higher frequencies, the noise source is more concentrated near the trailing edge, and the contribution from the wake region far from the trailing edge is very minimum (Wang and Moin 2000).

Scaling analysis of the spectra is carried out to study the dependence of vortex shedding noise on the Mach number and characteristic length and is plotted in Fig. 9 for different serration wavelengths. The sound pressure levels scaled with the flow velocity and the root thickness as the characteristic length is shown in Eq. (4) (Brooks and Marcolini 1985)

$$SPL_{\text{Scaled}} = 10\log_{10}\left(\frac{\overline{P^2}}{P_{\text{ref}}}\right) - n10\log_{10}M - 10\log_{10}\left(\frac{\varepsilon}{R}\right) \tag{4}$$

where $n$ = power law index; and $P_{\text{ref}} = 2 \times 10^{-5}$ Pa. Figs. 9(a–c) represents the normalized spectra of serrations with different wavelengths, and Figs. 9(d–f) represents the normalized spectra of serrations with different heights. The normalized spectra show a good collapse at the vortex shedding frequency range obtained within ±1 dB. Albeit the peak tonal frequency scales with the velocity and root thickness, the broadband noise in the frequency range of $1{,}350 \le f \le 5{,}000$ Hz does not scale with the parameters considered. It is interesting to note that in Fig. 9(a), the vortex shedding frequency region and the low frequency region prior to the vortex frequency ($300 \le f \le 600$ Hz) in the spectra coalesce fairly well for all velocities. This spectral collapse meant that the frequency components in this range have a fairly good dependence on the scaling parameters considered. However, an increase in serration wavelength shows that the spectra in the frequency zone failed to collapse well even though the root thickness is the same. This nature indicates that the noise components in the frequency range do not have a fair dependence on the scaling parameters, as shown in Figs. 9(b and c). The narrow serration shows a strong coherence of the vortex shedding, and this coherence alters the low frequency components and owing to the change in low frequency noise. On the contrary, the serration with a larger serration wavelength, the secondary flow between the serration tooth, and this flow alteration strongly affect the vortex shedding, which leads to the change in peak frequency and reduction in the peak noise levels. From Figs. 9(d–f) it is evident that even though the center frequency of the tone increases with a decrease in the serration height, it manifests fairly good collapse of the spectra in the frequency range $300 \le f \le 600$ Hz. It is also evident that the degree of coalescence increases with decrease in the serration height. The coalescing of the spectra in the frequency range $300 \le f \le 600$ Hz depicts the fact that increasing the height of the serration reduces the size of the vortices shed from the root, and they do not have enough strength to influence the upstream of the airfoil. Ultimately, this confirms that at higher frequencies, leading and trailing edge scattering are relatively independent (Wang and Moin 2000). Interestingly, the tonal amplitude is lowest for the smallest serration height [Fig. 9(f)] and the spectra is almost broadband. This is because, the shorter serrations have a smaller root thickness than their counterparts leading to a weaker vortex shedding.

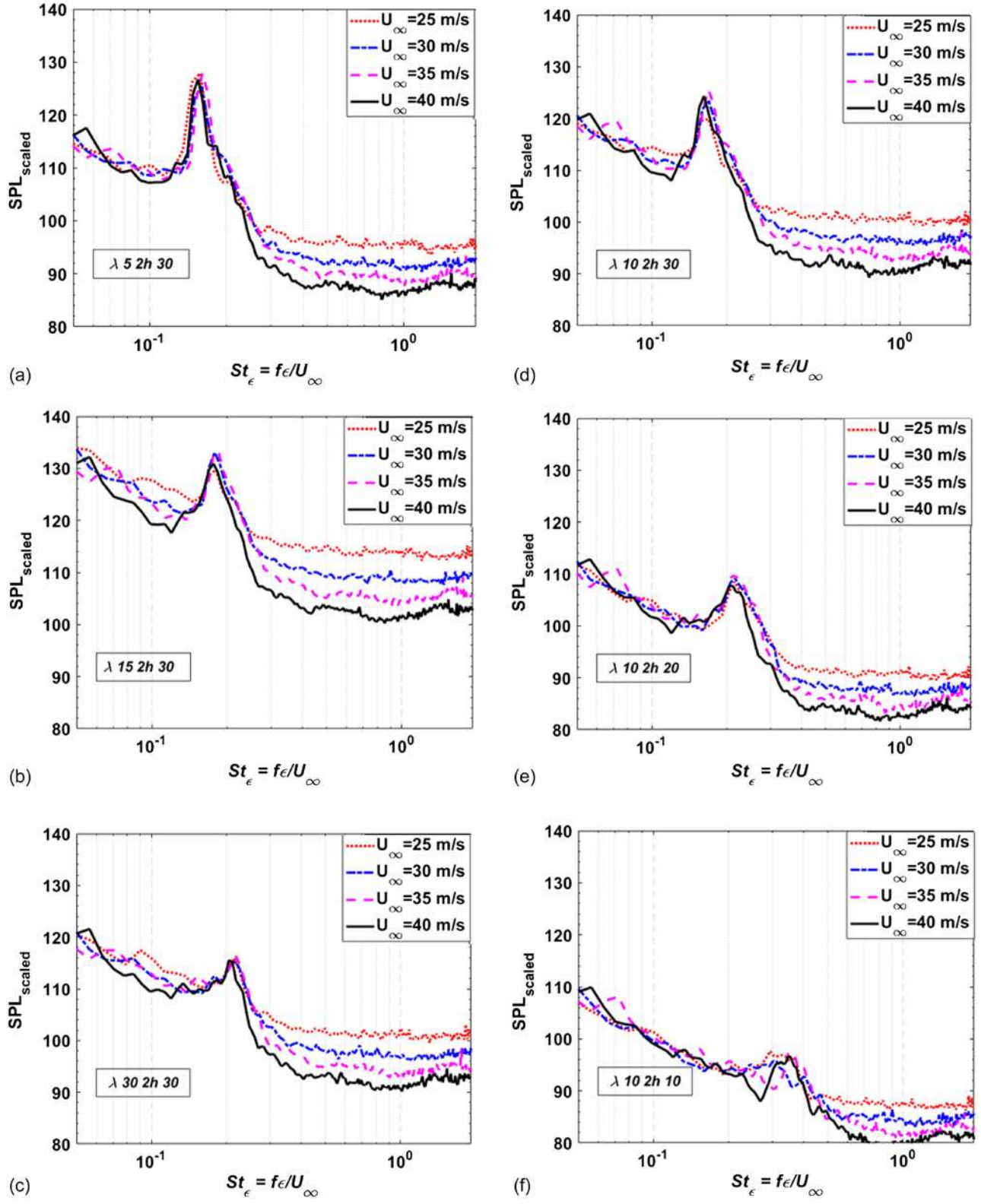


**Fig. 9.** Scaled acoustic spectra at different $U_\infty$ for different serrations.

Fig. 10(a) presents the scaling of the noise spectra of serrations of different $2h$ using the root thickness as the characteristic length. It is seen that the tonal frequency does not collapse well with root thickness. This may be due to the fact that tonal noise from the blunt trailing edge scales well with the wake thickness rather than the root thickness or boundary layer thickness alone, as discussed by Blake (1986). Therefore, an alternative scaling method that includes the root thickness and the displacement thickness ($\delta^*$) is adopted. For normalizing the spectra, Eq. (4) is modified with the quantity $(\varepsilon + 2\delta^*)$ and is shown in Eq. (5)

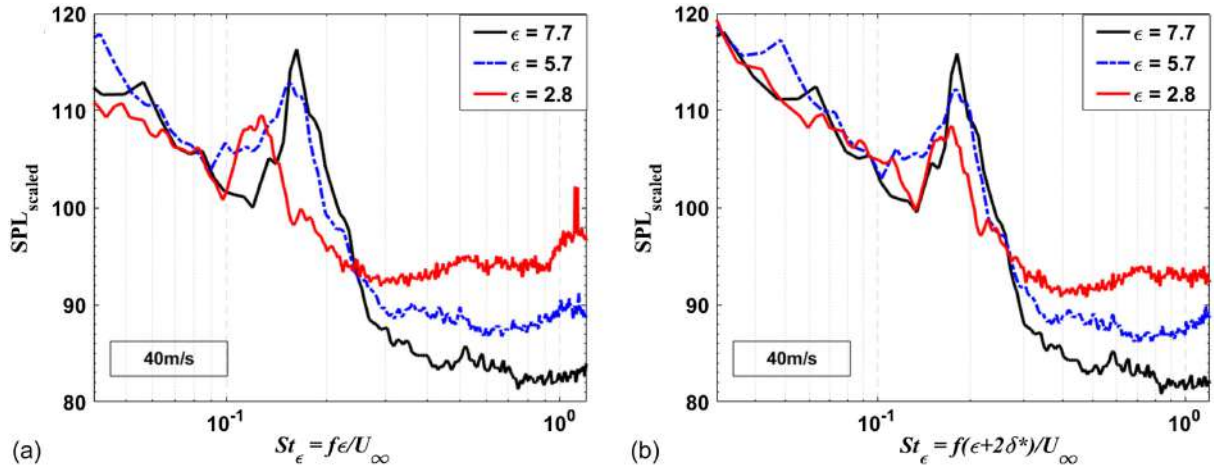


**Fig. 10.** Scaled acoustic spectra of blunt root serration using (a) $U_\infty$ and root thickness; and (b) $U_\infty$ and $\varepsilon + 2\delta^*$.

$$SPL_{\text{Scaled}} = 10\log_{10}\left(\frac{\overline{P^2}}{P_{\text{ref}}}\right) - n10\log_{10}M - 10\log_{10}\left(\frac{\varepsilon + 2\delta^*}{R}\right) \tag{5}$$

The displacement thickness over the airfoils at different flow velocities is estimated using the XFoil software version 6.99 (Drela 1989). It is noted that the low frequency region and the tonal noise in the spectra collapse well using the scaling parameter $\varepsilon + 2\delta^*$, as seen in Fig. 10(b). However, the slight deviation in the scaled amplitude in the spectra is due to the loss of strong coherence of the vortex due to three-dimensional flow through the serration root. Further, the high frequency TBL scattering noise does not show a good collapse. Fig. 11(a) depicts the variation of tonal peak frequency with flow velocity for serrations of different wavelengths and $2h = 30$. It can be noted that the tonal peak frequency increases with the flow velocity, and the corresponding slope scales with $U_\infty^{0.95}$. Fig. 11(b) shows tonal peak frequency variation with flow velocity for different serration heights and $\lambda = 10$. Results are found to be similar to that noticed in Fig. 11(a). Interestingly, the serration with lower root thickness ($2h = 10$) exhibits a different slope as compared to others [Fig. 11(b)] implying that the vortex shedding frequency varies with a higher exponent of velocity ($U_\infty^{1.3}$). It is also noted from Fig. 11 that the tonal frequency variation is linear for serrations of different wavelength and different heights.

The aforementioned section concludes that the serration made in the trailing edge of the airfoil has significant effects. Although it reduces the TBL scattering noise at higher frequencies, they tend to generate tones due to the root bluntness. Therefore, in the next section, modifications at the root are carried out that alter the vortex shedding and the resulting noise components.

### *Serrations with Modified Roots*

This section discusses the noise characteristics of different serration airfoils, which were modified to minimize the vortex shedding tonal noise. In the first modification, the root of the serration was gradually made to zero thickness by giving an inclination, as shown in Fig. 3(b). An airfoil with serration height of $2h = 30$ mm and $\lambda = 5$ mm was considered for further modifications. The inclinations provided at the root ($\theta$) were $\theta = 23°$ and $40°$ with the flow direction. The acoustic spectra of these serrations are shown in Fig. 12. The serration with $\theta = 40°$ shows a tonal frequency peak

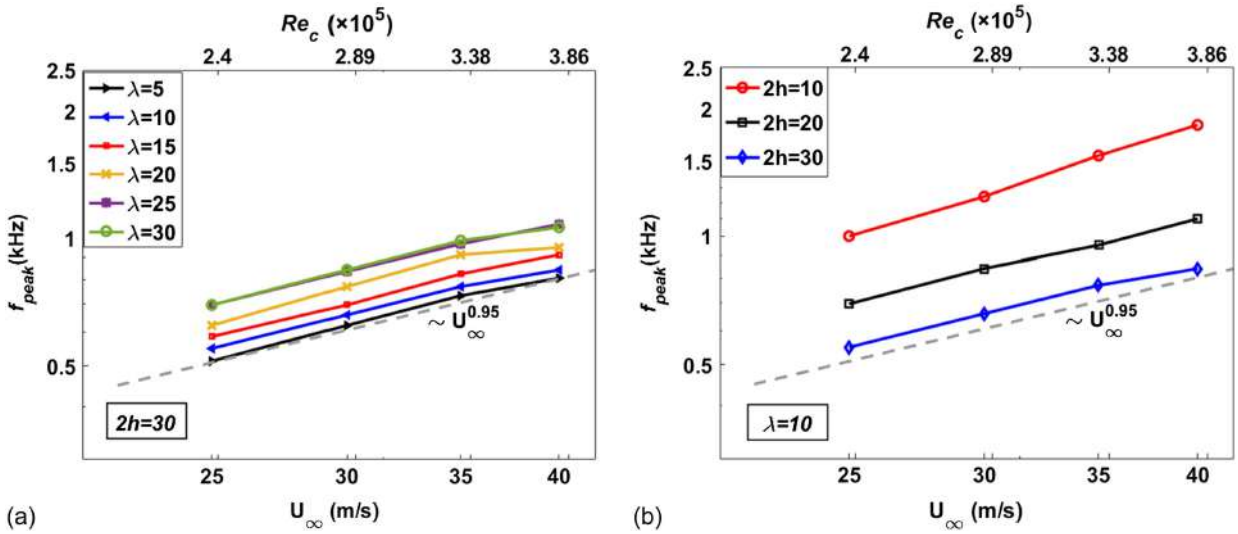


**Fig. 11.** Variation of peak frequencies with velocity and Reynolds number for (a) $2h = 30$ and different $\lambda$; and (b) $\lambda = 10$ and different $2h$.

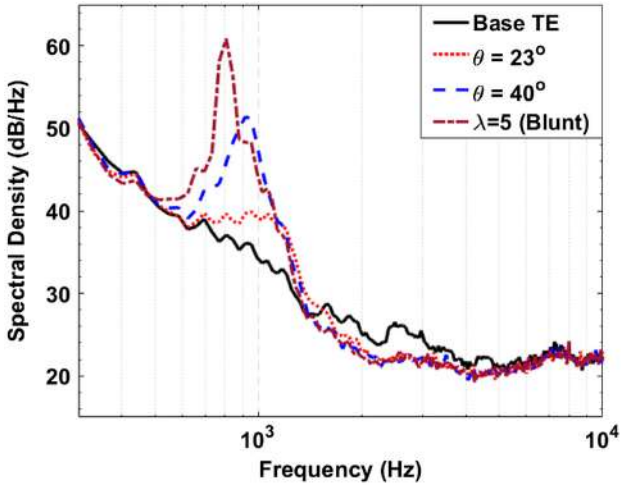


**Fig. 12.** Spectra of inclined serration of different values of $\theta$ for $\lambda = 5$ at $U_\infty = 40$ m/s.

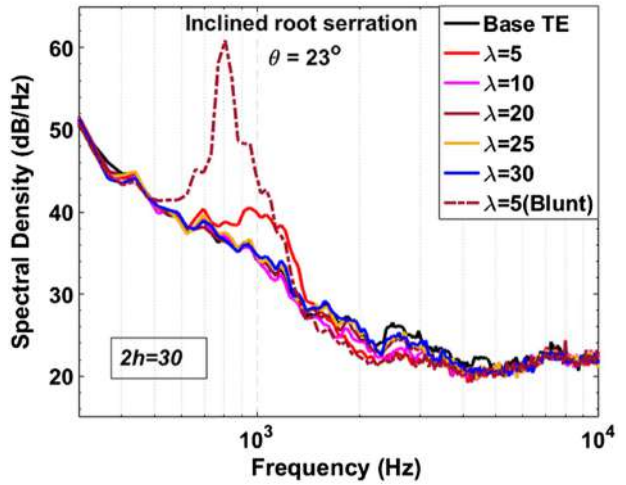


**Fig. 13.** Spectral comparison of different inclined root serrations with blunt root serration at $U_\infty = 40$ m/s.

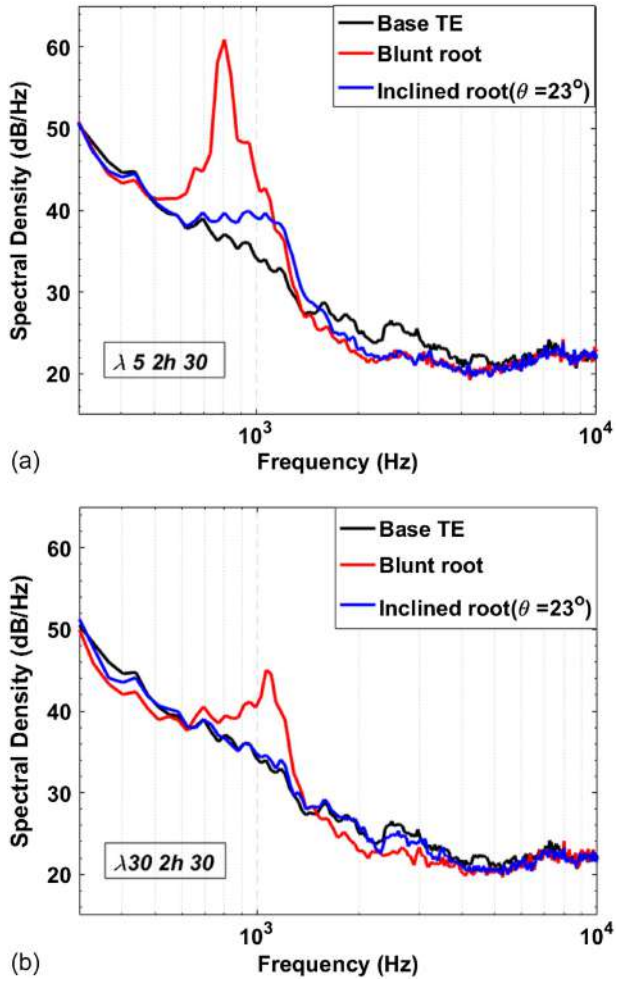


**Fig. 14.** Spectra comparison of blunt and inclined root serrations at $U_\infty = 40$ m/s: (a) serration with $\lambda 5\, 2h\, 30$; and (b) serration with $\lambda 30\, 2h\, 30$.

at a slightly higher frequency, around 900 Hz, as compared to the blunt root. However, the former is noted to have a noise reduction of up to 9 dB compared to the latter. The serration with $\theta = 23°$ has generated no tonal noise, and a reduction of around 22 dB is observed. However, the high frequency TBL scattering noise reduction is the same as that of the blunt root serration.

Fig. 13 presents the spectra of the serration with inclined root for different wavelengths and height of $2h = 30$. A broad hump can be observed in the spectra of the $\lambda = 5$ wavelength serration in the frequency range of $600 < f < 1{,}500$ Hz, which is greater than that of the base model airfoil. All other serrations models produce the same noise levels as the baseline case. However, in the TBL frequency range, a maximum reduction of 4.3 dB can be observed. The spectral comparison of the blunt root serration and inclined root serration having the same $\lambda$ and $2h$ is presented in Fig. 14. Fig. 14(a) shows the spectra of the shortest wavelength ($\lambda = 5$), and Fig. 14(b) shows the largest wavelength ($\lambda = 30$) serrations at a free stream velocity of 40 m/s. The inclined root with $\lambda =$ 5 mm characterized by a comparatively small broadband hump in the same frequency range of the vortex shedding noise of the blunt root serration. The high frequency broadband noise reduction obtained is not much adversely affected by the inclined root serration. On the other hand, when the wavelength of the serration increases, the broadband hump is completely eliminated but losses its advantage in the edge scattering noise. In the frequency range of $1{,}350 \le f \le 5{,}000$ Hz, corresponding to trailing edge scattering noise, the inclined root serrations generate the same noise levels as the baseline airfoil. This is because the root and the tip of the inclined root serrations are sufficiently sharp so that it efficiently scatters the vortices past the trailing edge with the same efficiency as that of a straight sharp trailing edge. Another idea adopted to eliminate the narrow band frequency due to the longitudinal vortex shedding at the serration roots was to insert a perforated plate in between the serration gaps along the span. Fig. 15 shows the noise spectra of baseline and blunt root with a perforated plate inserted airfoils. It is observed that the serrated trailing edge with a perforated insert reduces the noise levels in the frequency range of $300 < f < 780$ Hz. A maximum of 6.5 dB reduction in noise is observed in this frequency range. In general, the low frequency noise in this range can be attributed to the large-scale turbulent structures in the flow. Thus, the base airfoil is observed to have a larger noise in this frequency range (Fig. 15). However, in the airfoil with perforated plates, a cross flow is introduced, which interacts with the mainstream flow. This leads to the breakdown of large-scale turbulent structures to small-scale, thus, decreasing the noise levels in

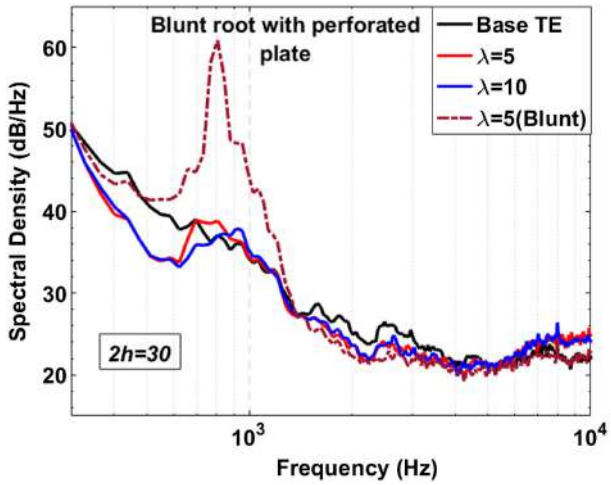


**Fig. 15.** Spectra comparison of blunt serrations with serration with perforated plate insert at $U_\infty = 40$ m/s.

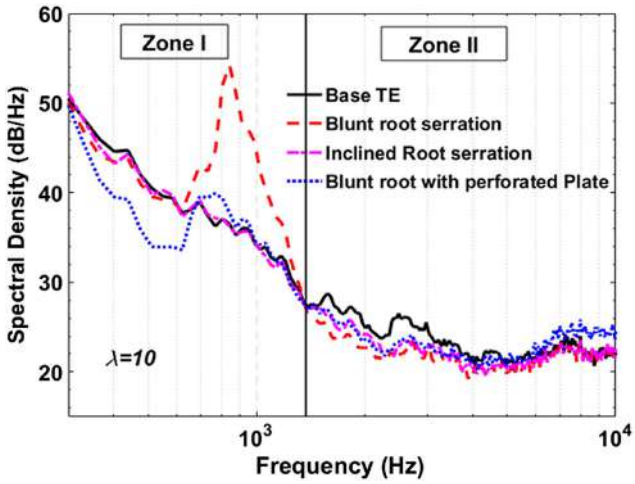


**Fig. 16.** Spectra at $U_\infty = 40$ m/s for straight and modified trailing edges.

this frequency range (Shahzad et al. 2022). In addition, there is no appreciable narrowband noise components in the spectra and are completely eliminated by the perforated inserts, as shown in Fig. 15. This indicates that the vortex shedding at the roots is prevented by the perforated plate. It is also noted that the maximum level of noise reduction for the narrow ($\lambda = 5$) and wide ($\lambda = 10$) serrations are the same (about 6 dB). The serrations with a perforated plate demonstrate not only its ability to eliminate the vortex shedding noise but also the turbulent broadband noise levels (Fig. 15). The level of broadband noise reduction is the same for both serrations ($\lambda = 5$ and $\lambda = 10$). However, it is interesting to note that when compared to the baseline case, the noise levels produced by the serration with a perforated plate increase at high frequencies beyond 6 kHz. The increase of noise at high frequencies is due to the roughness offered by the perforated plate.

### *Sound Pressure Level Comparison of Different Serrations*

In order to compare the noise level produced by the three serrations, the acoustic spectra of serrations $\lambda = 10$ wavelength and $2h = 30$ at a velocity of 40 m/s are plotted in Fig. 16. The figure indicates that the serrations have a significant effect on the radiated noise. Among these modifications, the perforated plate inserted at the blunt roots is more effective compared to other modifications. The modification achieved a reduction of around 6 dB in the low frequency range and around 4 dB reduction in the boundary layer scattering noise compared to the base model airfoil. In the figure, it is evident that different modifications give different noise levels at various frequency ranges. For detailed analysis, the SPL plot is divided into two frequency regions based on the spectra of baseline trailing edge and blunt trailing edge serration. Zone I is selected such that it is comprised of the low frequency region ($300 \le f \le 1{,}350$ Hz) just after the occurrence of the tonal noise. In zone II, a reduction in the broadband trailing edge noise can be observed within the frequency band ($1{,}350$ Hz $\le f \le 10$ kHz). The frequency zones are depicted in Fig. 16. The SPL of different zones is calculated by integrating the mean square pressure over the specific frequency range of different zones. The $\Delta$SPL of the frequency zone is obtained by subtracting the average sound pressure level of the modified airfoil from the base airfoil across the same frequency range.

Figs. 17(a and b) compares the difference in integrated SPL ($\Delta$SPL) over the frequency range defined by different zones of the blunt root serrations serration at different velocities. In Zone I, due to the presence of the tone, negative $\Delta$SPL is obtained, which represents the noise increase as compared to the baseline airfoil. Also, a decrease in $\Delta$SPL with an increase in the wavelength of the serration can be observed in Zone I. In Zone II, all the serrations show an average noise reduction of 5 dB at all velocities. Figs. 17(c and d) presents $\Delta$SPL variation of inclined root serration with velocity. The figure depicts that in zone I, the serration with the lowest serration angle ($\lambda 5\, 2h\, 30$) produces higher negative $\Delta$SPL at all velocities due to the vertex shedding at the roots of the serration. It is also noted that the difference in $\Delta$SPL tends to decrease with an increase in velocity. This might be due to the interaction of the secondary flow through the roots at higher velocities which disturbs the strong coherence of the vortex shedding at the toot and hence reduce the vortex shedding noise levels (Thomareis and Papadakis 2017). However, in zone II, all the serrations show positive $\Delta$SPL values at all velocities. It is also observed the noise reduction decreases with an increase in the velocity. An interesting thing to be noted is that the serration with the lowest value of $\lambda$, which generates higher noise levels in zone I, gives the largest broadband noise reduction in zone II. The reduction in broadband noise was found to be reduced with an increase in velocity for all serration types. Figs. 17(e and f) shows the noise reduction by the blunt serration with perforated plate insert across different zones. The SPL levels of only two serrations with different serration wavelengths were measured with a single perforated plate. This modification provides noise reduction in both zones at all velocities. In Zone I, both serrations generated noise levels lower than that of the base airfoil, and the wider serration generated more noise reduction. This is because the flow near the serration is more three-dimensional in the case of the wider serration as compared to that of sharper serration. The presence of a perforated plate in between the serration teeth collapses the large coherent structures, which are responsible for the low frequency noise. This alters the flow around the airfoil and helps to reduce the low frequency noise. The noise reduction is more or less the same at all velocities. Another thing to be noticed in Fig. 17(f) is that the broadband noise reduction in Zone II of the serration with a perforated plate insert is comparatively lesser as compared to other solid serrations considered. This is because the perforated plate brake down the large

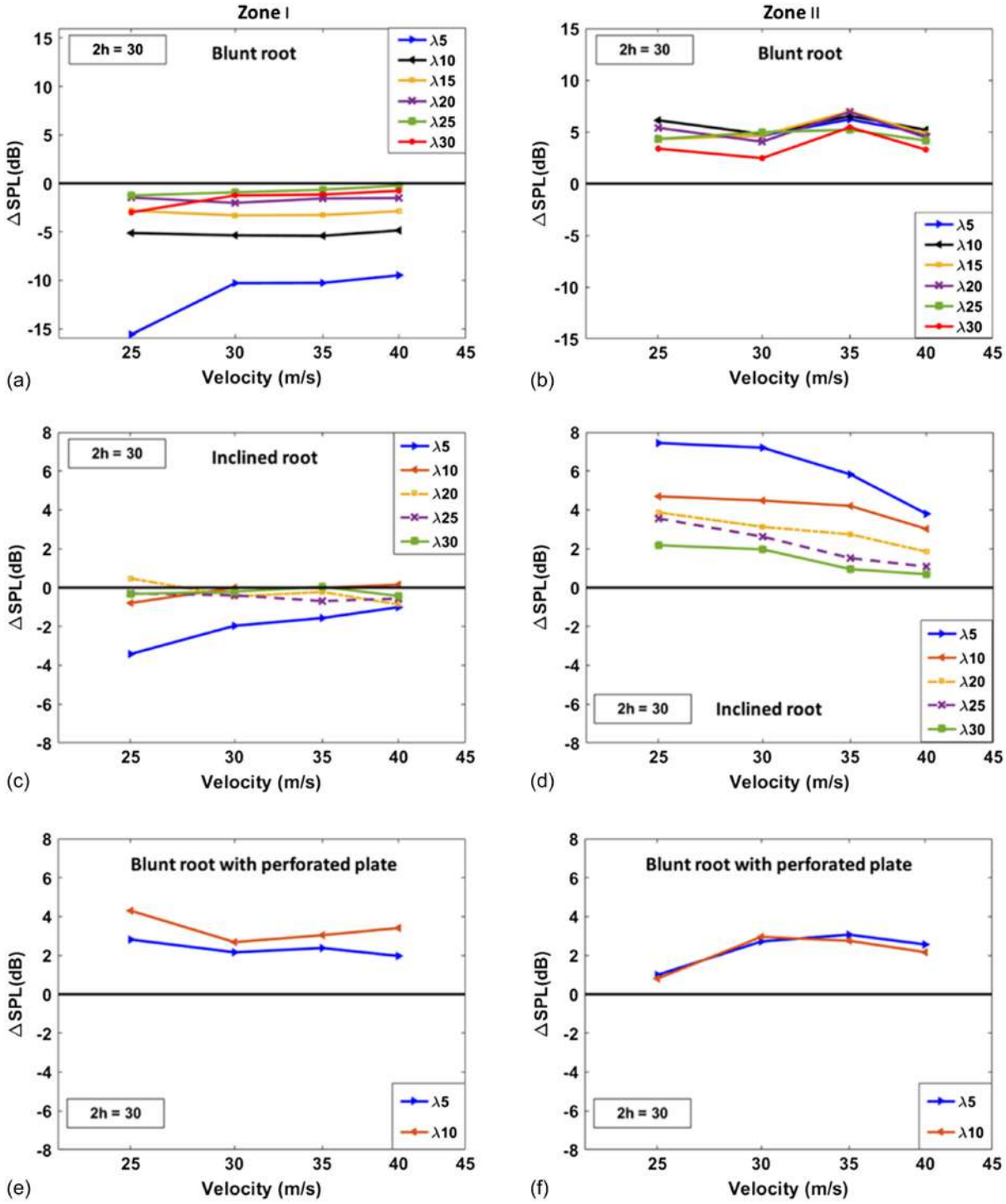


**Fig. 17.** Variation of ΔSPL of different serrations with mean flow velocity at different frequency zones of (a, c, and e) Zone I; and (b, d, and f) Zone II.

turbulent structures to a small-scale structure and its scattering tends to increase the high frequency broadband noise. The noise reduction increases with velocity, and a further increase in the velocity reduces the noise reduction due to the roughness noise of the perforated plate at high frequencies. The overall sound pressure level (OASPL) is calculated by integrating the same over the entire frequency range of 300 Hz to 10 kHz, using Eq. (6)

$$\mathrm{OASPL} = 10 \cdot \log_{10} \sum_{300\ \mathrm{Hz}}^{10\ \mathrm{kHz}} \left( \frac{\bar{p}_i^2}{p_{\mathrm{ref}}^2} \right) dB \tag{6}$$

The OASPL variation of different blunt root serration with mean flow velocity is shown in Fig. 18. In Fig. 18(a), it is seen that all cases of blunt serration exhibit higher noise levels as compared to the baseline case across all velocities. It is also observed that the serration with a lower serration wavelength ($\lambda = 5$) generates the highest noise level as compared to other models in all velocities due to the effect of strong vortex shedding at the serration roots. The dominance of the vortex shedding noise is shown to reduce with an increase in serration wavelength due to the reduction in the strength of the longitudinal vortex at the root. Fig. 18(a) also shows the velocity dependence of the overall noise levels of different blunt

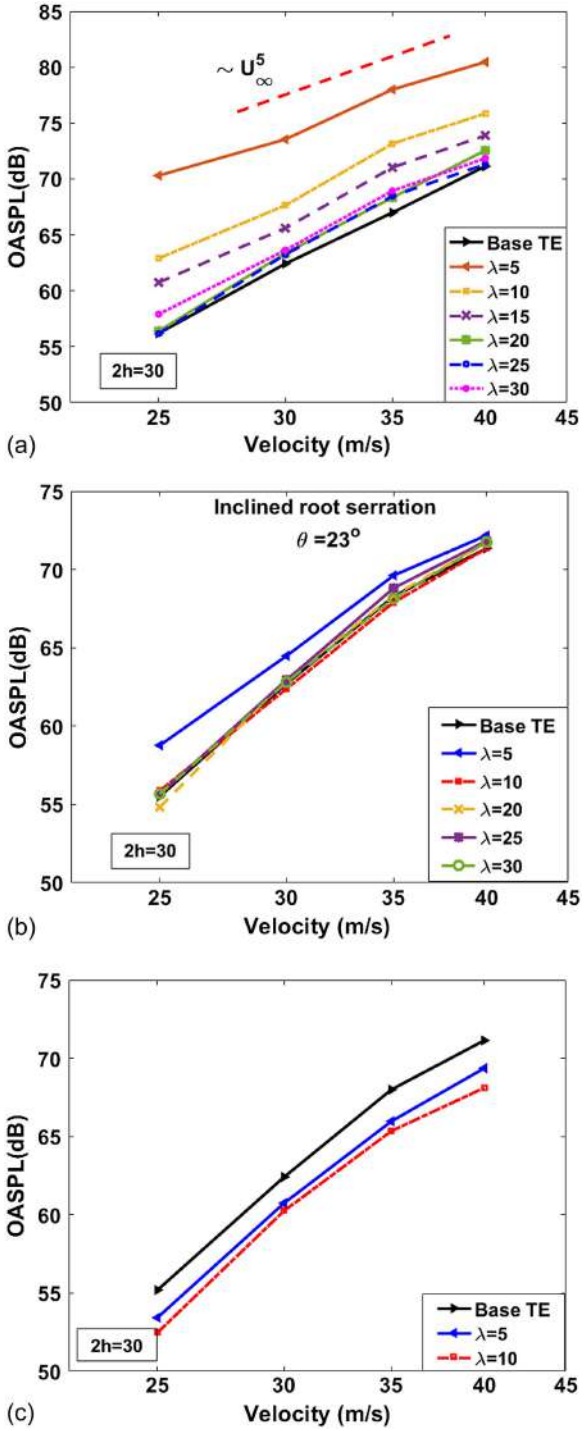


**Fig. 18.** Variation of OASPL with mean flow velocity of different root serrations: (a) blunt root; (b) inclined root; and (c) blunt root with perforated plate.

root serrations. Generally, the vortex shedding noise from cylinders and bluff bodies scales with sixth power of velocity while the airfoil tones scale with fifth power of velocity (Schlinker et al. 1976). In the Fig. 18(a), the OASPL of the serration with the lowest serration angle ($\lambda 5\, 2h\, 30$) shows a speed dependence of the fifth power of velocity ($\mathrm{OASPL}_{\lambda 5\, 2h\, 30} \propto U_\infty^5$), which corresponds to the airfoil vortex shedding noise (Schlinker et al. 1976). This reveals that the major contribution to the overall noise level is the vortex shedding noise as compared to other noise components. An interesting thing to be noted is that as the serration wavelength increases, the dependency of the OASPL with velocity is also varied, and a gradual shift from fifth power to seventh power dependency can be observed. This indicates that even though the vortex shedding noise is present in the spectra, its strength is considerably lower than that of the serration $\lambda 5\, 2h\, 30$, and other noise components, such as scattering noise and turbulent wake noise might be contributed to the overall noise levels. This variation in the velocity scaling is in congruence with the results of Schlinker et al. (1976). The serration with the largest serration angle, the OASPL varies with seventh power of the velocity demonstrates that the vortex shedding at the blunt root is highly inhibited by the secondary flow at the roots, and now the dominant noise sources become the quadruple noise sources at the wake and roots of the serration. The variation of OASPL with the velocity of the inclined root serration is shown in Fig. 18(b). It is observed that the OASPL of the sharper serration ($\lambda 5\, 2h\, 30$) is higher than the baseline case because the advantage of broadband noise reduction is nullified by the tonal noise due to the vortex shedding. Fig. 18(c) shows the overall noise levels of the blunt serration with a perforated plate. It shows a significant noise reduction over the entire velocity range considered. The wider serration with a perforated plate gives more reduction as compared to the narrow one.

## Conclusions

This paper reports the aerodynamic noise reduction achieved by airfoils with different nonflat plate serrations provided at the trailing edge of a NACA 0012 airfoil and its characteristics. The objective of the paper is to characterize noise from a conventional saw tooth nonflat plate serration and investigate whether the modification at the serration root geometry is feasible to employ to reduce both vortex shedding noise and broadband noise formed by the airfoil trailing edge. The blunt root serration employed at the trailing edge cause a large noise increase because of the vortex shedding at the roots of the serration. The vortex shedding noise level is found to decrease with an increase in serration wavelength; on the other hand, the peak frequency shifts to the higher side with an increase in serration wavelength. The frequency scaling analysis shows that the vortex shedding frequency does not scale properly as that of a blunt trailing edge due to the loss of coherence due to the cross flow at the serration gaps. The frequency ranges in which the vortex shedding noise was present was observed to scale with the scaling parameter $\varepsilon + 2\delta^*$ rather than the root thickness alone. However, variation in the scaling of the amplitude of the tones because of the different flow field of each of the serrations. Although the blunt root serration made at the trailing edge of the airfoil causes extraneous tones, it is capable of reducing the broadband noise by around 5 dB due to the lower scattering at the sawtooth tip. Since the vortex shedding noise nullifies the effect of broadband noise reduction, three serration models were considered to suppress the flow mechanism of vortex shedding at the roots. One with inclined root, the second with a perforated plate between the serration. All these modifications are found to be effective in eliminating the extraneous vortex shedding noise and obtaining significant broadband noise reduction up to 5–6 dB. The inclined root serration with the lowest serration wavelength provides the highest broadband (1.5–5 kHz) noise reduction (6 dB). Even though the noise reduction at the broadband range by the serration with perforated plate is lower as compared to other modifications, it is capable of producing around 7 dB reduction in Zone I. This modification shows a noise increase at higher frequencies due to the roughness offered by the perforated plates. However, 2–5 dB overall noise

reduction can be attained by this at all velocities. Considering all the serration geometries, serrations with smaller wavelength ($\lambda = 5$) are likely to produce maximum noise reduction in the broadband frequency (1.5–5 kHz) region at all velocities.

## Data Availability Statement

Some or all data, models, or code that support the findings of this study are available from the corresponding author upon reasonable request.

## References


Arce León, C., D. Ragni, S. Pröbsting, F. Scarano, and J. Madsen. 2016. "Flow topology and acoustic emissions of trailing edge serrations at incidence." *Exp. Fluids* 57 (91): 1–17. https://doi.org/10.1007/s00348-016-2181-1.

Arias Ramírez, W., and W. R. Wolf. 2015. "Effects of trailing edge bluntness on airfoil tonal noise at low Reynolds numbers." *J. Braz. Soc. Mech. Sci. Eng.* 38 (8): 2369–2380. https://doi.org/10.1007/s40430-015-0308-6.

Avallone, F., S. Pröbsting, and D. Ragni. 2016. "Three-dimensional flow field over a trailing-edge serration and implications on broadband noise." *Phys. Fluids* 28 (11): 117101. https://doi.org/10.1063/1.4966633.

Blake, W. K. 1986. *Mechanics of flow induced sound and vibration*. Orlando, FL: Academic Press.

Brooks, T. F., and M. A. Marcolini. 1985. "Scaling of airfoil self-noise using measured flow parameters." *AIAA J.* 23 (2): 207–213. https://doi.org/10.2514/3.8896.

Brooks T. F., D. S. Pope, and M. A. Marcolini. 1989. *Airfoil self-noise and prediction*. NASA Reference Publication 1218. Hampton, VA: NASA Langley Research Center.

Celik, A., Y. D. Mayer, and M. Azarpeyvand. 2021. "On the aeroacoustic characterization of a robust trailing-edge serration." *Phys. Fluids* 33 (7): 19–26. https://doi.org/10.1063/5.0054767.

Chen, N., H. Liu, Q. Liu, and Y. Wang. 2021. "Wake modification and noise emission of serrated NACA 65(12)-10 at moderate Reynolds number." *J. Aerosp. Eng.* 34 (5): 04021056. https://doi.org/10.1061/(ASCE)AS.1943-5525.0001299.

Chong, T. P., and E. Dubois. 2016. "Optimization of the poro-serrated trailing edges for airfoil broadband noise reduction." *J. Acoust. Soc. Am.* 140 (2): 1361–1373. https://doi.org/10.1121/1.4961362.

Chong, T. P., P. F. Joseph, and M. Gruber. 2013a. "Airfoil self noise reduction by non-flat plate type trailing edge serrations." *Appl. Acoust.* 74 (4): 607–613. https://doi.org/10.1016/j.apacoust.2012.11.003.

Chong, T. P., and A. Vathylakis. 2015. "On the aeroacoustic and flow structures developed on a flat plate with a serrated sawtooth trailing edge." *J. Sound Vib.* 354 (Jun): 65–90. https://doi.org/10.1016/j.jsv.2015.05.019.

Chong, T. P., A. Vathylakis, P. F. Joseph, and M. Gruber. 2013b. "Self-noise produced by an airfoil with nonflat plate trailing-edge serrations." *AIAA J.* 51 (11): 2665–2677. https://doi.org/10.2514/1.J052344.

Dassen, T., R. Parchen, J. Bruggeman, and F. Hagg. 1996. "Results of a wind tunnel study on the reduction of airfoil self-noise by the application of serrated blade trailing edges." In *Proc., the European Union Wind Energy Conf. and Exhibition*. Gothenburg, Sweden: European Commission and Göteborg Energi AB.

Drela, M. 1989. "XFOIL: An analysis and design system for low Reynolds number airfoils." In Vol. 54 of *Proc., Conf. on Low Reynolds Number Aerodynamics*. Berlin: Springer.

Giguere, P., and M. S. Selig. 1999. "Aerodynamic effects of leadingedge tape on aerofoils at low Reynolds numbers." *Wind Energy* 2 (3): 125–136. https://doi.org/10.1002/(SICI)1099-1824(199907/09)2:3<125::AID-WE23>3.0.CO;2-5.

Gruber, M., P. F. Joseph, and T. P. Chong. 2010. "Experimental investigation of airfoil self noise and turbulent wake reduction by the use of trailing edge serrations." In *Proc., 16th AIAA/CEAS Aeroacoustics Conf.* Stockholm, VA: American Institute of Aeronautics and Astronautics.

Gruber, M., P. F. Joseph, and T. P. Chong. 2011. "On the mechanisms of serrated airfoil trailing edge noise reduction." In *Proc., 17th AIAA/CEAS Aeroacoustics Conf. 2011 (32nd AIAA Aeroacoustics Conf.)*. Portland, VA: American Institute of Aeronautics and Astronautics.

Hasheminasab, S. M., S. M. H. Karimian, S. Noori, M. Saeedi, and C. Morton. 2021. "Experimental investigation of the wake dynamics for a NACA0012 airfoil with a cut-in serrated trailing-edge." *Phys. Fluids* 33 (5): 1–18. https://doi.org/10.1063/5.0046318.

Hasheminejad, S. M., T. P. Chong, P. F. Joseph, and G. Lacagnina. 2018. "Airfoil self-noise produced by fractal-serrated trailing edge." In *Proc., 24th AIAA/CEAS Aeroacoustics Conf.* Atlanta: American Institute of Aeronautics and Astronautics.

Howe, M. S. 1976. "The influence of vortex shedding on the generation of sound by convected turbulence." *J. Fluid Mech.* 76 (4): 711–740. https://doi.org/10.1017/S0022112076000864.

Howe, M. S. 1991. "Aerodynamic noise of a serrated trailing edge." *J. Fluids Struct.* 5 (1): 33–45. https://doi.org/10.1016/0889-9746(91)80010-B.

Hu, Y. S., P. J. Y. Zhang, Z. H. Wan, N. S. Liu, D. J. Sun, and X. Y. Lu. 2022. "Effects of trailing-edge serration shape on airfoil noise reduction with zero incidence angle." *Phys. Fluids* 34 (10): 105108. https://doi.org/10.1063/5.0108565.

Inasawa, A., C. Ninomiya, and M. Asai. 2013. "Suppression of tonal trailing-edge noise from an airfoil using a plasma actuator." *AIAA J.* 51 (7): 1695–1702. https://doi.org/10.2514/1.J052203.

Liu, X., H. Kamliya Jawahar, M. Azarpeyvand, and R. Theunissen. 2017. "Aerodynamic performance and wake development of airfoils with serrated trailing-edges." *AIAA J.* 55 (11): 3669–3680. https://doi.org/10.2514/1.J055817.

Lyu, B., M. Azarpeyvand, and S. Sinayoko. 2016. "Prediction of noise from serrated trailing edges." *J. Fluid Mech.* 793 (Jun): 556–588. https://doi.org/10.1017/jfm.2016.132.

Moreau, D. J., and C. J. Doolan. 2013. "Noise-reduction mechanism of a flat-plate serrated trailing edge." *AIAA J.* 51 (10): 2513–2522. https://doi.org/10.2514/1.J052436.

Nedić, J., and J. C. Vassilicos. 2015. "Vortex shedding and aerodynamic performance of airfoil with multiscale trailing-edge modifications." *AIAA J.* 53 (11): 3240–3250. https://doi.org/10.2514/1.J053834.

Oerlemans, S., M. Fisher, T. Maeder, and K. Kögler. 2009. "Reduction of wind turbine noise using optimized airfoils and trailing-edge serrations." *AIAA J.* 47 (6): 1470–1481. https://doi.org/10.2514/1.38888.

Parchen, R., W. Hoffmans, A. Gordner, and K. Braun. 1999. "Reduction of airfoil self-noise at low Mach number with a serrated trailing edge." In *Proc., 6th Int. Congress on Sound and Vibration*. Auburn, AL: International Institute of Acoustics and Vibration.

Powell, A. 1959. "On the aerodynamic noise of a rigid flat plate moving at zero incidence." *J. Acoust. Soc. Am.* 31 (12): 1649–1653. https://doi.org/10.1121/1.1907674.

Prigent, S. L., O. R. H. Buxton, and P. J. K. Bruce. 2017. "Coherent structures shed by multiscale cut-in trailing edge serrations on lifting wings." *Phys. Fluids* 29 (7): 075107. https://doi.org/10.1063/1.4995467.

Schlinker, R., M. R. Fink, and R. Amiet. 1976. "Vortex noise from nonrotating cylinders and airfoils." In *Proc., 14th Aerospace Sciences Meeting*. Washington, DC: American Institute of Aeronautics and Astronautics.

Shahzad, H., S. Hickel, and D. Modesti. 2022. "Permeability and turbulence over perforated plates." *Flow Turbul. Combust.* 109 (4): 1241–1254. https://doi.org/10.1007/s10494-022-00337-7.

Singh, S. K., M. Garg, S. Narayanan, L. Ayton, and P. Chaitanya. 2022. "On the reductions of airfoil broadband noise through sinusoidal trailing-edge serrations." *J. Aerosp. Eng.* 35 (2): 1–21. https://doi.org/10.1061/(ASCE)AS.1943-5525.0001386.

Sumesh, C. K., and T. J. S. Jothi. 2021. "Aerodynamic noise from an asymmetric airfoil with perforated extension plates at the trailing edge." *Int. J. Aeroacoust.* 20 (1–2): 88–108. https://doi.org/10.1177/1475472X20978388.

Szoke, M., D. Fiscaletti, and M. Azarpeyvand. 2020a. "Influence of boundary layer flow suction on trailing edge noise generation." *J. Sound Vib.* 475 (Jun): 115276. https://doi.org/10.1016/j.jsv.2020.115276.

Szoke, M., D. Fiscaletti, and M. Azarpeyvand. 2020b. "Uniform flow injection into a turbulent boundary layer for trailing edge noise reduction." *Phys. Fluids* 32 (8): 085104. https://doi.org/10.1063/5.0013461.

Tam, C. K. W., and H. Ju. 2012. "Aerofoil tones at moderate Reynolds number." *J. Fluid Mech.* 690 (Feb): 536–570. https://doi.org/10.1017/jfm.2011.465.

Thomareis, N., and G. Papadakis. 2017. "Effect of trailing edge shape on the separated flow characteristics around an airfoil at low Reynolds number: A numerical study." *Phys. Fluids* 29 (1): 1–17. https://doi.org/10.1063/1.4973811.

van der Velden, W. C. P., F. Avallone, and D. Ragni. 2017. "Numerical analysis of noise reduction mechanisms of serrated trailing edges under zero lift condition." In *Proc., 23rd AIAA/CEAS Aeroacoustics Conf.* Denver: American Institute of Aeronautics and Astronautics.

Vathylakis, A., T. P. Chong, and P. F. Joseph. 2015. "Poro-serrated trailing-edge devices for airfoil self-noise reduction." *AIAA J.* 53 (11): 3379–3394. https://doi.org/10.2514/1.J053983.

Vathylakis, A., T. P. Chong, C. Paruchuri, and P. F. Joseph. 2016. "Sensitivity of aerofoil self noise reductions to serration flap angles." In *Proc., 22nd AIAA/CEAS Aeroacoustics Conf*. Lyon, VA: American Institute of Aeronautics and Astronautics.

Wang, M., and P. Moin. 2000. "Computation of trailing-edge flow and noise using large-eddy simulation." *AIAA J.* 38 (12): 2201–2209. https://doi.org/10.2514/2.895.

Williams, J. E. F., and L. H. Hall. 1970. "Aerodynamic sound generation by turbulent flow in the vicinity of a scattering half plane." *J. Fluid Mech.* 40 (4): 657–670. https://doi.org/10.1017/S0022112070000368.